Downloaded from ascelibrary.org by Hong Kong University of Sci and Tech (HKUST) on 06/05/19. Copyright ASCE. For personal use only; all rights reserved.

Transient Frequency Responses for Pressurized Water Pipelines Containing Blockages with Linearly Varying Diameters

T. C. Che[1]; H. F. Duan, M.ASCE[2]; P. J. Lee[3]; B. Pan[4]; and M. S. Ghidaoui, M.ASCE[5]

Abstract: Extended partial blockages in urban water supply systems (UWSS) are formed from complicated physical, chemical, and biological processes; thus, these blockages are commonly in random and nonuniform geometries. The transient-based blockage detection method (TBBDM) has been evidenced in many applications to be a promising way to diagnose these blockages. Despite the successful validation and application of the TBBDM in the literature, pipe blockages used in these studies were idealized and simplified to regular and uniform shape, which are however not common in practical UWSS, and thus invalidity and inaccuracy of this TBBDM has been widely observed in practical applications. This paper presents fundamental research on understanding the influence of more realistic and nonuniform blockages on transient wave behavior and the accuracy of current TBBDM. The blockage with a linearly varying diameter (termed as nonuniform blockage) is firstly investigated by the frequency domain analytical analysis for its impact on transient wave behavior, which is thereafter incorporated in the overall transfer matrix of transient frequency response for reservoir-pipeline-valve systems. The results indicate the nonuniform blockage may induce very different modification patterns on the frequency shift and amplitude change of transient waves from the uniform blockage situation. **DOI: 10.1061/(ASCE)HY.1943-7900.0001499.** *© 2018 American Society of Civil Engineers.*

Author keywords: Nonuniform blockage; Water pipelines; Transient; Frequency response; Transfer matrix.

Introduction

Blockages commonly exist in pressurized fresh water and seawater conveying pipelines due to various physical, chemical, and biological processes, including corrosion, biofilm accumulation, and deposition of sediments. Blockages can reduce pipe diameters and increase pipe wall roughness, resulting in lower water carrying capacity, additional energy loss, and deterioration of water quality (James and Shahzad 2003). Unlike leaks, blockages are masked in the inaccessible buried pipeline network because they lack external evidence needed for detection and the lost pressure and flow across the blockage can be compensated by other branch pipelines in the network (Stephens 2008). Therefore, it is crucial to develop a nondestructive blockage detection method to reduce the impact of blockages on the urban water supply systems (UWSS).

A variety of pipeline fault (leakage and blockage) detection methods has been summarized by Datta and Sarkar (2016), among which the transient-based method (Colombo et al. 2009; Lee et al. 2013) is thought to be a promising way for diagnosing pipeline faults because it has the desirable merits of high efficiency, low cost, and nondestructive applications. The principle of this method is that pipeline faults can be detected by inducing a transient pressure wave into the pipeline followed by measuring and analyzing the pressure wave echoes (transient responses) from the potential pipe faults. Localized pipe faults (such as leaks and discrete blockages) generate additional pressure signals within the transient response; therefore, the location of these localized faults can be determined based on the occurrence time of the first pressure signal and the system wave speed. The transient-based analysis approach has been developed and used by many researchers for detecting and locating different localized pipe faults in the time domain (Brunone 1999; Brunone and Ferrante 2001; Covas and Ramos 2010; Covas et al. 2004; Lee et al. 2007; Meniconi et al. 2010, 2011). Although it is easy to operate, the small reflected pressure signal from localized faults is easily interfered by random background noise, making it difficult to accurately identify. Moreover, the complexity of system connections (such as multiple-pipe systems) may cause technical trouble for separating the transient response information (e.g., reflection) of faults from other sources when using this time-domain method. To address this problem, a number of publications proposed spectral analysis as an alternative way for detecting and sizing different localized faults in the frequency domain (Brunone and Ferrante 2004; Ferrante and Brunone 2003; Gong et al. 2014; Kim 2017; Lee et al. 2006, 2008, 2015; Sattar and Chaudhry 2008; Wang et al. 2005).

Specifically, Lee et al. (2006) showed that the presence of leaks in a pipeline induces a sinusoidal fluctuation pattern (termed the leak-induced pattern) onto the resonance peaks, and the amplitude and shape of this leak-induced pattern can be used to detect the size and location of the leak. It was also found that resonance peaks of

[1]Ph.D. Student, Dept. of Civil and Environmental Engineering, Hong Kong Polytechnic Univ., Hung Hom, Kowloon, Hong Kong SAR, P.R. China. Email: tong-chuan.che@connect.polyu.hk

[2]Assistant Professor, Dept. of Civil and Environmental Engineering, Hong Kong Polytechnic Univ., Hung Hom, Kowloon, Hong Kong SAR, P.R. China (corresponding author). Email: hf.duan@polyu.edu.hk

[3]Professor, Dept. of Civil and Natural Resources Engineering, Univ. of Canterbury, Private Bag 4800, Christchurch, New Zealand. Email: pedro.lee@canterbury.ac.nz

[4]Ph.D. Student, Dept. of Civil and Environmental Engineering, Hong Kong Polytechnic Univ., Hung Hom, Kowloon, Hong Kong SAR, P.R. China. Email: bin.pan@connect.polyu.hk

[5]Chair and Professor, Dept. of Civil and Environmental Engineering, Hong Kong Univ. of Science and Technology, Kowloon, Hong Kong SAR, P.R. China. Email: ghidaoui@ust.hk

Note. This manuscript was submitted on August 16, 2017; approved on March 12, 2018; published online on June 14, 2018. Discussion period open until November 14, 2018; separate discussions must be submitted for individual papers. This paper is part of the ***Journal of Hydraulic Engineering***, © ASCE, ISSN 0733-9429.

leak case are in the same position as the leak-free case; in other words, no shifting of the frequency peaks is imposed. Discrete blockages in pipelines were found to have a similar influence on the resonant peaks (Lee et al. 2008; Sattar et al. 2008); therefore, the size and location of discrete blockage can be diagnosed using a similar approach. Brunone et al. (2008) showed that extended blockages, which is a common scenario in aging pipelines, have a totally different influence on transient responses from discrete blockages, and thus methods used for discrete blockage detection may not be applicable to extended blockages. Duan et al. (2012) showed that extended blockages not only change the amplitude of resonant peaks, but also induce frequency shifts in resonant peaks (termed as blockage-induced frequency shifts). On the basis of the derived wave-blockage dispersion relationship in Duan et al. (2012), a genetic algorithm (GA) based inverse optimization procedure was proposed to determine the physical properties (such as length, size, and location) of potential extended blockages. Duan et al. (2014) further inspected the transient wave-blockage interaction and theoretically explained the aforementioned blockage-induced frequency shifts.

Despite the successful application of this transient-based method for extended blockage detection in many numerical and laboratory tests, blockages used for analysis in previous studies were idealized and simplified to uniform shapes (Duan et al. 2012, 2014; Lee et al. 2013; Louati et al. 2017; Meniconi et al. 2013; Rubio Scola et al. 2017; Tuck et al. 2013), which are actually equivalent to multiple pipe sections in series with different diameters connected together. However, real world blockages that are often formed from complex sources and processes are usually in highly random and nonuniform shapes as illustrated in Figs. 1(a–c). Recently, Duan et al. (2017) experimentally investigated the influence of nonuniform blockages on transient wave behavior and the validity of current transient-based method for nonuniform blockage detection. It has been found that the blockage nonuniformity may have a great impact on both the wave attenuation and the phase (frequency) shift, which causes invalidity and inaccuracy of the current transient-based method when it is used to detect these nonuniform blockages. Therefore, a further, in-depth understanding of the influence of nonuniform blockages on transient responses is important for the development of a more accurate blockage detection method for practical UWSS.

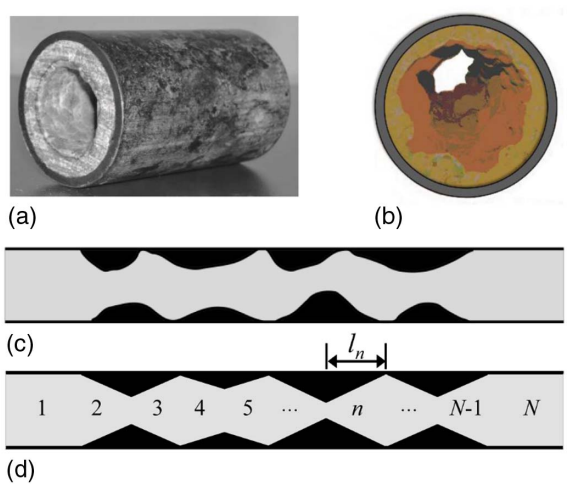

Fig. 1. (a) Severe blockages in urban water pipelines (reprinted from Meniconi et al. 2013, © ASCE); (b) nonuniform blockages in practical water pipelines (adapted from James and Shahzad 2003); (c) sketch of realistic pipeline with nonuniform blockages; and (d) sketch of pipeline with nonuniform blockages used for quantitative analysis.

To study the modification effect of nonuniform blockages on the system frequency response, Chaudhry (2014) replaced the actual nonuniform blockage (i.e., pipeline with gradually varying diameter) by a number of substitute uniform blockages in series. This treatment discretized the nonuniform blockage into many pricewise constant elements, and then individual matrixes for each element were multiplied to produce the approximated overall matrix for the whole nonuniform blockage. From their results, this approximation method only gives satisfactory prediction for the first few harmonic modes, and it is computationally expensive to get relatively accurate results for higher harmonic modes. As a result, this approximation treatment method may induce potential errors and influences for the transient modeling and utilization such as pipe blockage detection, especially for a pipeline with multiple blockages (Duan et al. 2010). Therefore, it is worthwhile to develop more reliable (more accurate and efficient) methods to describe the transient frequency response of realistic blockage situations in water pipelines.

As a preliminary study, it is preferable and feasible to examine the realistic cases of nonuniform blockages by starting with simple cases, such as blockages with linearly varying diameters (termed as nonuniform blockages in this study) as shown in Fig. 1(d), with the aim to understand the fundamental physics and mechanism of wave-blockage interactions. Specifically, the transient wave behavior in a single nonuniform blockage is obtained by analytically solving the wave equation under specific initial and boundary conditions. Thereafter, the obtained wave solutions are used to derive the overall transfer matrix for water pipeline systems with nonuniform blockages. The derived transfer matrix is fully validated by the traditional method of characteristics (MOC), and then used to systematically investigate the influences of nonuniform blockage shape, severity, and length on transient frequency responses. Finally, the findings and practical implications of this study are discussed.

Models and Methods

Wave Equation for a Single Nonuniform Blockage

The one-dimensional (1D) wave equation for nonuniform blockages with varying cross-sectional areas was derived as (Duan et al. 2011; Duan 2017)

$$A\frac{\partial^2 P}{\partial t^2} = a^2\frac{\partial}{\partial x}\left(A\frac{\partial P}{\partial x}\right) \tag{1}$$

where t = time; x = axial coordinate along the pipeline; $A = A(x)$ = pipe cross-sectional area; P = instantaneous pressure in the time domain; and $a = a(x)$ = acoustic wave speed, which represents the characteristics of pipe-wall deformation and properties of internal fluid (e.g., water).

Note that a frictionless pipeline system with elastic pipe wall is firstly considered in the analytical derivation to highlight the wave-blockage interaction (Duan et al. 2014). Pipeline systems with linearized steady friction will be further discussed in the numerical applications.

Alternatively, Eq. (1) can be rewritten

$$\frac{\partial^2 P}{\partial t^2} - a^2\frac{\partial^2 P}{\partial x^2} = a^2\frac{A'}{A}\frac{\partial P}{\partial x} \tag{2}$$

where A' = derivative dA/dx. For transient pipe flows, the instantaneous pressure P can be expressed as (Chaudhry 2014)

Downloaded from ascelibrary.org by Hong Kong University of Sci and Tech (HKUST) on 06/05/19. Copyright ASCE. For personal use only; all rights reserved.

$$P = P_0 + p^* \tag{3}$$

where P_0 = mean pressure; and p^* = pressure deviation from the mean. Because the pipeline is frictionless, P_0 is constant in terms of both x and t, and then Eq. (2) becomes

$$\frac{\partial^2 p^*}{\partial t^2} - a^2 \frac{\partial^2 p^*}{\partial x^2} = a^2 \frac{A'}{A} \frac{\partial p^*}{\partial x} \tag{4}$$

which is a linear partial differential equation (PDE) and can be solved under specific boundary and initial conditions.

Transient Wave Behavior in a Single Nonuniform Blockage

In the preceding wave equation, it is assumed that the solution p^* has the following form (Chaudhry 2014)

$$p^*(x,t) = p(x)e^{i\omega t} \tag{5}$$

where p = pressure in the frequency domain; ω = angular frequency; and i = imaginary part.

Substituting Eq. (5) back into Eq. (4), the PDE becomes the following linear ordinary differential equation (ODE)

$$\frac{d^2 p}{dx^2} + \frac{A'}{A}\frac{dp}{dx} + k^2 p = 0 \tag{6}$$

where $k = k(x) = \omega/a(x)$ = wave number. In fact, Eq. (6) is in the same form with the Webster's horn equation in acoustics (Webster 1919). The variation of the wave speed within a shallow nonuniform blockage along the axial direction is relatively small compared with the wave speed a_0 in intact sections. For example, the field tests by Lee et al. (2017) showed that the average percentage of wave speed variation in deteriorated field water pipelines is around 8.25%. Thus, the wave speed $a_b(x)$ within the nonuniform blockage is represented by the average value (i.e., $\bar{a}_b$) throughout the blockage section, which is different from the original value of intact pipelines (i.e., a_0) because of the blockage-induced changes in pipe properties (e.g., diameter, thickness, and material). As a result, the wave number k within the nonuniform blockage in Eq. (6) becomes $k_b = \omega/\bar{a}_b$. Sensitivity analysis will be conducted later in this paper to examine the validity range (limitation) of this assumption (i.e., using the average wave speed within the blockage section).

Applying Eq. (6) in the nth nonuniform blockage, as shown in Fig. 1(d), provides

$$\frac{d^2 p_n}{dx^2} + \frac{A_n'}{A_n}\frac{dp_n}{dx} + k_b^2 p_n = 0 \tag{7}$$

For quantitative analysis, the pipe radius of the nth nonuniform blockage in Fig. 1(d) is defined as

$$r_n(x) = s_n x + R_{Ln} \tag{8}$$

where r_n = pipe radius of the nth nonuniform blockage; R_{Ln} = pipe radius at the left boundary of the nth nonuniform blockage; and $s_n = (R - R_{Ln})/l_n$ = slope of the nth nonuniform blockage, in which R = intact pipe radius and l_n = length of the nth nonuniform blockage in Fig. 1(d).

Based on the expression of r_n in Eq. (8), the pipe cross-sectional area A_n and its derivative A_n' can be calculated, thus

$$\frac{A_n'(x)}{A_n(x)} = \frac{2s_n}{s_n x + R_{Ln}} \tag{9}$$

Substituting Eq. (9) into Eq. (7), it becomes

$$\frac{d^2 p_n}{dx^2} + \frac{2s_n}{s_n x + R_{Ln}}\frac{dp_n}{dx} + k_b^2 p_n = 0 \tag{10}$$

It is assumed that the solution for the wave equation Eq. (10) is a plane wave solution in the following form (Munjal 2014)

$$p_n = \frac{e^{\alpha x}}{r_n(x)} = \frac{e^{\alpha x}}{s_n x + R_{Ln}} \tag{11}$$

where α = coefficient that remains to be determined; note that the denominator is the pipe radius of the nth nonuniform blockage in Eq. (8). Furthermore, substituting Eq. (11) into Eq. (10) results in the following characteristic equation for α

$$\alpha^2 + k_b^2 = 0 \tag{12}$$

As a result, α has two solutions

$$\alpha_1 = ik_b, \qquad \alpha_2 = -ik_b \tag{13}$$

Substituting two solutions into Eq. (11), two special solutions for wave equation Eq. (10) can be obtained

$$(p_n)_1 = \frac{e^{ik_b x}}{s_n x + R_{Ln}}, \qquad (p_n)_2 = \frac{e^{-ik_b x}}{s_n x + R_{Ln}} \tag{14}$$

In fact, these two plane wave solutions $(p_n)_1$ and $(p_n)_2$ are the incident and reflected waves propagating toward opposite directions. It can be observed from the numerator of Eq. (14) that the transient waves distribute sinusoidally in space with a constant wave number k_b. In addition, the amplitude of these two waves is modified by the denominator, which is the pipe radius of the nth nonuniform blockage. It means that the wave amplitude is inversely proportional to the radius of the nth nonuniform blockage.

Because the wave equation Eq. (10) is a linear ODE, based on the superposition principle, the general solution for wave equation can be obtained

$$p_n = \frac{C_1 e^{ik_b x} + C_2 e^{-ik_b x}}{s_n x + R_{Ln}} \tag{15}$$

where C_1 and C_2 are two constants.

To have an intuitive sense of wave behavior in a single nonuniform blockage, the plane wave solutions in Eq. (14) are visualized in both uniform and nonuniform blockages. A localized incident wave is created at the right boundary of these two blocked pipelines, and detailed parameters of these two systems are listed in Table 1. Note that these two pipelines have the same blocked volume, which means that the average pipe diameter for these two blockages is the same, and the left boundaries of these two pipelines are reflection-free. The obtained results are plotted in Fig. 2, showing how the localized incident wave evolves as it propagates in the pipeline from right to left. The spatial coordinate x is

Table 1. Parameter settings for illustrative systems with uniform and nonuniform blockages

Type	l_n	s_n	R_{Ln}	k_b
Uniform blockage	$100R$	0	$0.9R$	$\pi/5$
Nonuniform blockage	$100R$	2×10^{-3}	$0.8R$	$\pi/5$

Downloaded from ascelibrary.org by Hong Kong University of Sci and Tech (HKUST) on 06/05/19. Copyright ASCE. For personal use only; all rights reserved.

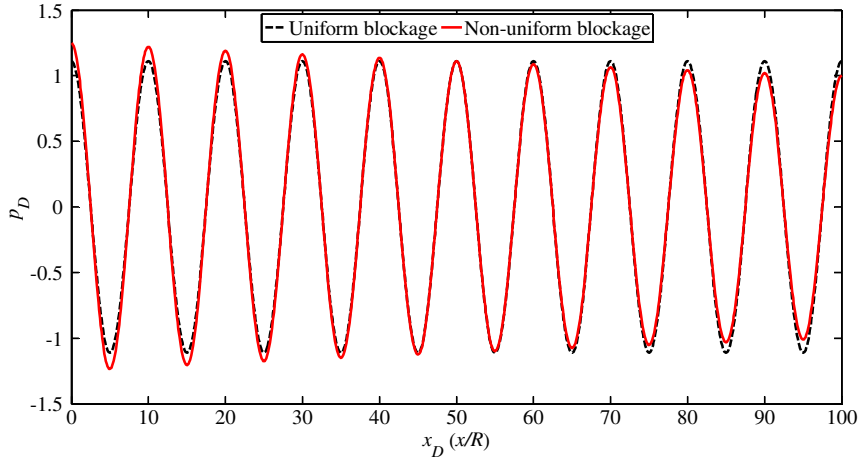

Fig. 2. Transient wave behavior in uniform and nonuniform blockages.

normalized by the intact pipe radius R and is expressed as x_D in the horizontal axis. The pressure is normalized by the pressure in the intact pipeline and is expressed as dimensionless pressure p_D.

It can be seen from Fig. 2 that the wave amplitude in the uniform blockage keeps constant, while the wave amplitude in the nonuniform blockage gradually increases as the wave propagates to the left. This is consistent with the wave solution in Eq. (14), because the denominator of Eq. (14) for the nonuniform blockage gradually decreases from right to left. In fact, this result is consistent with the former study by the authors with regard to energy analysis of wave scattering in disordered-diameter pipelines (Duan et al. 2011). That is, nonuniform blockages in the pipeline may cause the energy redistribution of pressure waves in both temporal and spatial domains in the system.

Overall Transfer Matrix for Pipeline Systems with a Single Nonuniform Blockage

To study the transient frequency responses for pipeline systems with a single nonuniform blockage, the obtained wave solution in Eq. (15) is used to derive the transfer matrix. The transfer matrix is the linearized counterpart of mass and momentum equations in the frequency domain. It describes the wave behavior and connects state vectors at two boundaries of the pipeline system without discretization of the pipeline in space. Thus, it has the advantage of computational efficiency compared with some time domain methods, such as the MOC.

The derivation procedure of the transfer matrix for a single uniform blockage (or pipeline) was provided in Chaudhry (2014). A similar procedure is adopted herein to derive the transfer matrix for a single nonuniform blockage, based on the wave solution in Eq. (15). Note that the pressure deviation p in Eq. (15) is transformed into the pressure head deviation h in this section, which is a common practice in hydraulic engineering.

The derived transfer matrix for a single nonuniform blockage [i.e., the nth nonuniform blockage in Fig. 1(d)] is

$$\begin{pmatrix} q \\ h \end{pmatrix}_{n+1} = \begin{pmatrix} U_{11} & U_{12} \\ U_{21} & U_{22} \end{pmatrix} \begin{pmatrix} q \\ h \end{pmatrix}_n \tag{16}$$

where q = discharge deviation in the frequency domain; h = pressure head deviation in the frequency domain; subscripts n and $n+1$ = upstream and downstream boundaries of the nth nonuniform blockage, respectively; and U_{ij} = elements of transfer matrix, with the following forms:

$$U_{11} = -\frac{iR_{Ln}}{2k_b(s_n l_n + R_{Ln})^2}\frac{A_{n+1}}{A_n}\{[ik_b(s_n l_n + R_{Ln}) - s_n]e^{ik_b l_n} + [ik_b(s_n l_n + R_{Ln}) + s_n]e^{-ik_b l_n}\}$$

$$U_{12} = -\frac{A_{n+1}g}{2\omega k_b(s_n l_n + R_{Ln})^2}\{[ik_b(s_n l_n + R_{Ln}) - s_n](ik_b R_{Ln} + s_n)e^{ik_b l_n} - [ik_b(s_n l_n + R_{Ln}) + s_n](ik_b R_{Ln} - s_n)e^{-ik_b l_n}\}$$

$$U_{21} = \frac{\omega R_{Ln}}{2k_b(s_n l_n + R_{Ln})A_n g}(e^{-ik_b l_n} - e^{ik_b l_n})$$

$$U_{22} = \frac{1}{2ik_b(s_n l_n + R_{Ln})}[(ik_b R_{Ln} + s_n)e^{ik_b l_n} + (ik_b R_{Ln} - s_n)e^{-ik_b l_n}]$$

Note that the uniform blockage is a special case of the nonuniform blockage when the slope s_n equals zero ($s_n = 0$). As a result, Eq. (16) becomes

$$\begin{pmatrix} q \\ h \end{pmatrix}_{n+1} = \begin{pmatrix} \cos(k_0 l_n) & -i\dfrac{1}{M_{n+1}}\sin(k_0 l_n) \\ -iM_n \sin(k_0 l_n) & \cos(k_0 l_n) \end{pmatrix} \begin{pmatrix} q \\ h \end{pmatrix}_n \tag{17}$$

where k_0 = wave number for the uniform blockage; and $M_n = a/A_n g$. This result is consistent with the transfer matrix for a uniform blockage in Chaudhry (2014).

To study the transient frequency responses, the derived transfer matrix is applied to a reservoir-pipeline-valve (RPV) system as shown in Fig. 3. The transfer matrix with external head and discharge perturbations should be expanded to a 3×3 matrix in the following form (Chaudhry 2014; Duan et al. 2012; Lee et al. 2008)

$$\begin{pmatrix} q \\ h \\ 1 \end{pmatrix}_B = \begin{pmatrix} U_{11} & U_{12} & U_{13} \\ U_{21} & U_{22} & U_{23} \\ U_{31} & U_{32} & U_{33} \end{pmatrix} \begin{pmatrix} q \\ h \\ 1 \end{pmatrix}_A \tag{18}$$

where subscripts A and B = upstream and downstream boundaries of the pipeline system. Variables q_B and h_B at the downstream valve can be expressed as

Downloaded from ascelibrary.org by Hong Kong University of Sci and Tech (HKUST) on 06/05/19. Copyright ASCE. For personal use only; all rights reserved.

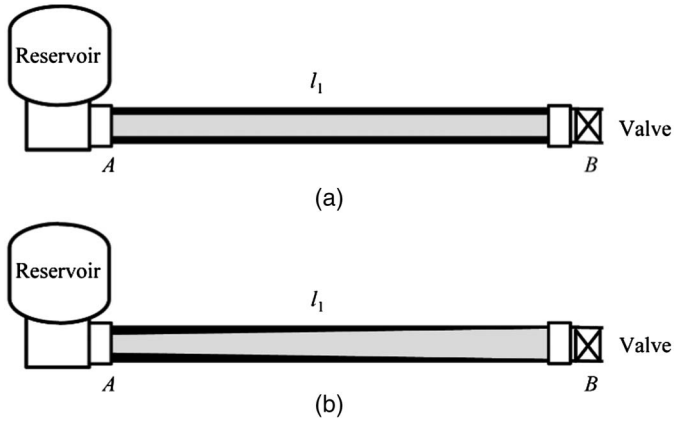

Fig. 3. Illustrative RPV systems with (a) single uniform blockage; and (b) single nonuniform blockage.

$$q_B = U_{11}q_A + U_{12}h_A + U_{13} \tag{19}$$

$$h_B = U_{21}q_A + U_{22}h_A + U_{23} \tag{20}$$

For the RPV system in Fig. 3, it has the boundary conditions $h_A = q_B = 0$. Eqs. (19) and (20) result in

$$h_B = \frac{U_{21}U_{13}}{U_{11}} + U_{13} \tag{21}$$

As a result, for a leak-free pipeline system, Eq. (21) becomes (Lee et al. 2006)

$$h_B = -\frac{U_{21}}{U_{11}} \tag{22}$$

The resonant frequency of head responses for RPV systems with a single nonuniform blockage can be obtained when the denominator of Eq. (22) (i.e., U_{11}) equals to zero.

For RPV systems with a single uniform blockage, ($n = 1$ and $s_1 = 0$), the resonance frequency is

$$U_{11} = \cos(k_0 l_1) = 0 \tag{23}$$

which shows that the resonant peaks are uniformly distributed in the frequency domain.

Similarly, for RPV systems with a single nonuniform blockage, ($n = 1$ and $s_1 \neq 0$), let $U_{11} = 0$, resulting in the resonant frequency for this RPV system

$$k_b(s_1 l_1 + R_{L1})\cos(k_b l_1) - s_1 \sin(k_b l_1) = 0 \tag{24}$$

Unlike the resonant frequency for the uniform blockage, Eq. (24) has an extra term $\sin(k_b l_1)$, which may result in resonant frequency shifts. If the slope of this nonuniform blockage equals zero (i.e., $s_1 = 0$), the nonuniform blockage becomes a uniform blockage and Eq. (24) becomes $\cos(k_b l_1) = 0$. This result indicates that resonant peaks for a uniform blockage are uniformly distributed regardless of the radius size, which is consistent with Eq. (23).

The transient frequency responses for an RPV system are studied for both uniform and nonuniform blockages. Note that the friction is neglected herein for highlighting the effect of blockage nonuniformity. As shown in Fig. 3, there is a single blockage (uniform or nonuniform) between the upstream reservoir and downstream valve. The transient wave is caused by the fast and full closure of the downstream valve.

The frequency responses for both cases are plotted in Fig. 4. The frequency is normalized by the fundamental frequency of the pipeline system $\omega_{th} = \bar{a}_b/4l_1$, and is expressed as nondimensional frequency ω^*. Theoretically the amplitude of head response should go to infinity because the friction is not included in the transfer matrix. It is shown in Fig. 4 that the resonant peaks for the uniform blockage are uniformly distributed, whereas that for the nonuniform blockage has evident frequency shifts, especially for the first resonant peak. Moreover, as the frequency increases, the induced frequency shift by the nonuniform blockage becomes less evident. This can be explained by the analytical resonant frequency in Eq. (24): as frequency increases, the wave number k_b also increases, then the first term $\cos(k_b l_1)$ in Eq. (24) will become dominant; therefore, the frequency shift caused by the nonuniform blockage becomes less evident for higher frequency modes.

Extended Transfer Matrix for Pipeline Systems with Multiple Nonuniform Blockages

So far, the transfer matrixes for single uniform and nonuniform blockages have been obtained. For illustration and simplification, only the case of two joint nonuniform blockages shown in Fig. 5(b) is considered and investigated in this study, although for more complex cases a similar analysis procedure presented herein can

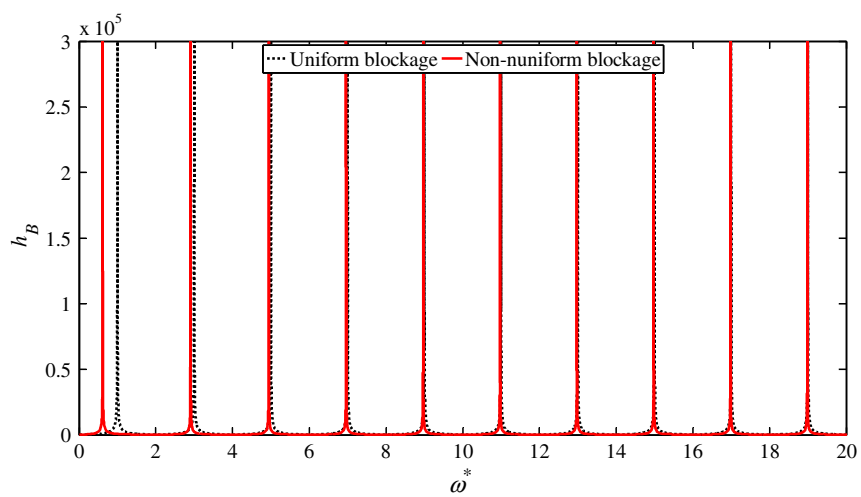

Fig. 4. Transient frequency responses for RPV systems with single uniform and nonuniform blockages (without friction effect).

Downloaded from ascelibrary.org by Hong Kong University of Sci and Tech (HKUST) on 06/05/19. Copyright ASCE. For personal use only; all rights reserved.

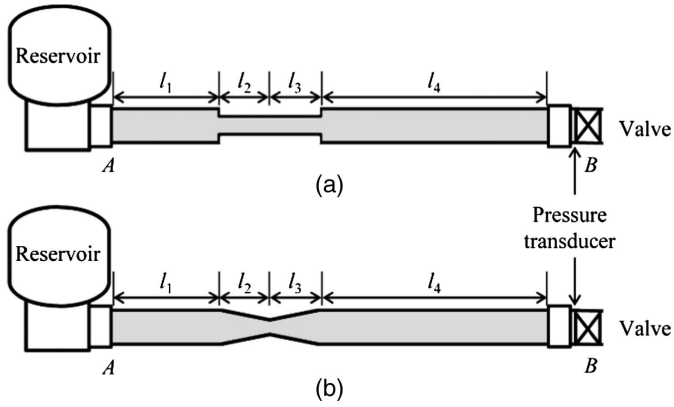

Fig. 5. Illustrative RPV systems with (a) uniform blockages; and (b) nonuniform blockages.

be applied. It is assumed there is no pressure head loss at pipe junctions (Duan et al. 2012). The overall matrix for this pipeline system (made up of four segments) relates the state vectors at two boundaries, A and B, and can be obtained by multiplying individual matrixes for each pipe element in the order of their locations starting from the downstream end

$$\begin{Bmatrix} q \\ h \end{Bmatrix}_B = \begin{bmatrix} \cos(k_0 l_4) & -i\dfrac{1}{M_4}\sin(k_0 l_4) \\ -iM_4 \sin(k_0 l_4) & \cos(k_0 l_4) \end{bmatrix} \times \begin{bmatrix} U_{11} & U_{12} \\ U_{21} & U_{22} \end{bmatrix}_3 \times \begin{bmatrix} U_{11} & U_{12} \\ U_{21} & U_{22} \end{bmatrix}_2 \times \begin{bmatrix} \cos(k_0 l_1) & -i\dfrac{1}{M_1}\sin(k_0 l_1) \\ -iM_1 \sin(k_0 l_1) & \cos(k_0 l_1) \end{bmatrix} \begin{Bmatrix} q \\ h \end{Bmatrix}_A \tag{25}$$

For clarity, Eq. (25) can be further derived and written

$$\begin{Bmatrix} q \\ h \end{Bmatrix}_B = \begin{bmatrix} U_{11}^* & U_{12}^* \\ U_{21}^* & U_{22}^* \end{bmatrix} \begin{Bmatrix} q \\ h \end{Bmatrix}_A \tag{26}$$

where U_{ij}^* = elements of the overall transfer matrix for the four-pipeline system.

Similar with Eqs. (23) and (24), the resonance frequency for the four-pipeline system can be obtained by letting

$$U_{11}^* = 0 \tag{27}$$

Note that the analytical result in Eq. (27) for resonant frequency of a four-pipeline system becomes complicated in its mathematical expression, which can be obtained by solving the former Eqs. (16) and (25). Compared with the intact PRV system, the resonant frequency shift of Eq. (27) can be attributed to two sources: (1) the blockage nonuniformity $A(x)$ and (2) the wave speed nonuniformity $a(x)$ along the axial direction of the PRV system. To highlight the influence of blockage nonuniformity (or to eliminate the influence of wave speed nonuniformity) on resonant frequency shifts and simplify the analytical derivation in Eq. (27), it is first assumed herein that the wave speed in the whole pipeline system is constant, and the absolute values of nonuniform blockage slope $|s_2|$ (constriction section) and $|s_3|$ (expansion section) in Fig. 5(b) are equal ($|s_2| = |s_3| = s$). Then, Eq. (27) becomes

$$4R^2 R_{L3}\omega^3 \cos[k_b(l_1 + l_2 + l_3 + l_4)] + \sum a^f s^f \omega^{3-f} F^{3-f}(R, R_{L3}) \sin[k_b(l_1 \pm l_2 \pm l_3 \pm l_4)] = 0 \tag{28}$$

where the second term on the left-hand side contains a series of trigonometric terms; $F()$ = linear function of R and R_{L3}; f = integer ranges from 1 to 3. Three special cases are firstly verified as follows:

1. $s = 0$ (i.e., blockage-free case): the pipe radius on the left boundary of second pipeline in Fig. 5(b) R_{L2} is the same as the intact pipe radius R; $s = 0$ means that there is no blockage in the four-pipeline system. All terms containing s equal zero, and only one term $4R^2 R_{L3}\omega^3 \cos[k_b(l_1 + l_2 + l_3 + l_4)] = 0$ does not contain s. Under this condition, Eq. (28) is simplified into

$$\cos[k_b(l_1 + l_2 + l_3 + l_4)] = 0$$

which implies that the resonant peaks for the intact four-pipeline system of Fig. 5(b) are uniformly distributed in the frequency domain, which is consistent with previous studies (Chaudhry 2014; Lee et al. 2013).

2. $s \sim \infty((l_2 + l_3)/(l_1 + l_2 + l_3 + l_4) \sim 0$, i.e., discrete blockage case): if the slope of the nonuniform blockage tends to infinity, it means that the length of the nonuniform blockage is negligibly small compared with the total length of the pipeline $(l_2 + l_3)/(l_1 + l_2 + l_3 + l_4) \sim 0$, and the nonuniform blockage can be regarded as a discrete blockage. Terms with s to the high order will become dominant, but the summation of all terms containing s^3 equals zero. Therefore, all terms containing s^2 are further summed, and it turns out to be

$$\cos[k_b(l_1 + l_4)] = 0$$

Because the blockage length $l_2 + l_3$ is negligibly small compared with the total length of the pipeline $l_1 + l_2 + l_3 + l_4$, the preceding equation can be approximated by $\cos[k_b(l_1 + l_2 + l_3 + l_4)] = 0$. This is equivalent to the former results for the blockage-free case ($s = 0$) and indicates that the discrete blockage does not induce frequency shifts, which is well verified by the known results from previous studies (Lee et al. 2008, 2013).

3. High-frequency harmonic waves: the terms in the equation with the highest order of ω will play dominant roles. Only the term $4R^2 R_{L3}\omega^3 \cos[k_b(l_1 + l_2 + l_3 + l_4)] = 0$ contains ω^3; therefore, Eq. (28) is simplified into

$$\cos[k_b(l_1 + l_2 + l_3 + l_4)] = 0$$

which is the same as the blockage-free case ($s = 0$). It means that the frequency shift induced by the blockage nonuniformity becomes less evident as the frequency increases. It is a reminder that this result and analysis here is obtained under the condition of constant wave speed in the whole pipeline system, and the influence of wave speed variation from the blockage section is inspected in the following study.

Numerical Validation

To validate the analytical resonant frequency in Eq. (27), the classical frictionless 1D water hammer model coupling with the MOC is adopted herein for comparison. The RPV system with two joint nonuniform blockages is used for the numerical validation. In this study, nonuniform blockages are represented by stainless-steel pipelines with linearly varying diameters as shown

Downloaded from ascelibrary.org by Hong Kong University of Sci and Tech (HKUST) on 06/05/19. Copyright ASCE. For personal use only; all rights reserved.

Table 2. Parameter settings for numerical validation

Blockage type	l_1 (m)	l_2 (m)	l_3 (m)	l_4 (m)	R (m)	s	R_{L3} (m)	a_0 (m/s)	$\bar{a}_b$ (m/s)
Nonuniform	295	105	105	495	0.25	0.1/105	0.15	1,000	1,050

in Fig. 5(b). The original intact stainless-steel pipeline ($R = 0.25$ m, $L = 1{,}000$ m) is blocked by nonuniform blockages with minimum radius $R_{L3} = 0.15$ m and $l_2 = l_3 = 105$ m (refer to Table 2 for detailed parameters). Wave speeds for intact and blocked pipe sections are calculated based on the wave speed formula given in Wylie et al. (1993) and Chaudhry (2014) as $a_0 = 1{,}206$ and $\bar{a}_b = 1{,}249$ m/s. For simplicity of MOC calculation, a_0 and $\bar{a}_b$ are taken to be 1,000 and 1,050 m/s, respectively. In the numerical simulation, the nonuniform blockage is approximated by stepwise discretized grids, and the 1,000-m-long pipeline is divided into 3,960 relatively small reaches (i.e., spatial grid size $\Delta x \sim 0.25$ m) to decrease the frequency shift caused by numerical errors. The transient (pressure wave) is generated by a sudden and full closure of the downstream valve, and the pressure head trace is measured at the upstream face of the valve. The measured pressure head trace is transformed into the frequency domain by a fast Fourier transform (FFT) algorithm.

The analytical and numerical transient frequency responses with the first 10 resonant peaks are plotted in Fig. 6(a). In addition, the resonant frequency difference between analytical and numerical MOC results for the first 100 resonant peaks are extracted and plotted in Fig. 6(b). Fig. 6(a) shows that the resonant peaks for the nonuniform blockage system are not uniformly distributed, and this means the presence of the nonuniform blockages has changed the resonant frequencies of the original intact system. Moreover, these figures indicate good agreement between the analytical and numerical results in terms of resonant frequency, which confirms the validity of the analytical result in Eq. (27).

Further Application and Results Analysis

Based on the validated overall transfer matrix, the transient frequency responses for RPV systems with nonuniform blockages, as shown in Fig. 5(b), are investigated in this section. Duan et al. (2012) demonstrated that friction effects (both steady and unsteady) induce decreases in the magnitude of resonant peaks but have little impact on the location of resonant peaks, and the main purpose of

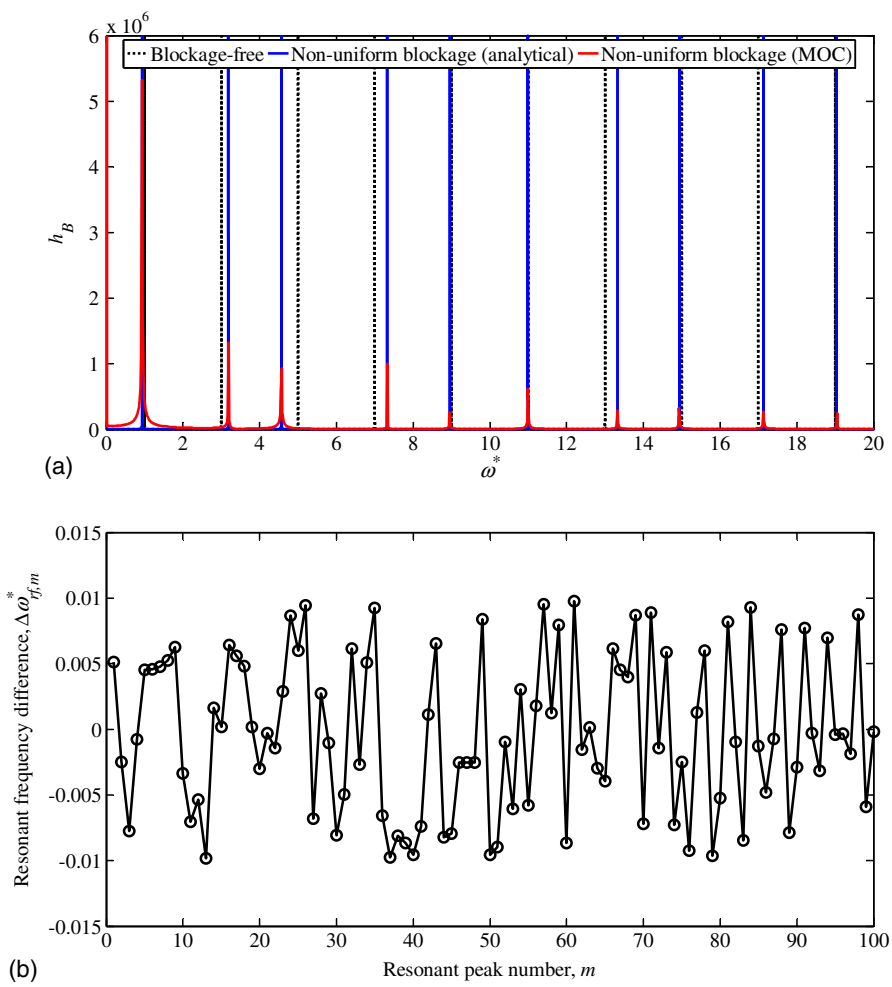

Fig. 6. Comparison of analytical and numerical results without friction effect: (a) transient frequency responses; (b) resonant frequency difference between analytical and numerical MOC results.

Downloaded from ascelibrary.org by Hong Kong University of Sci and Tech (HKUST) on 06/05/19. Copyright ASCE. For personal use only; all rights reserved.

Table 3. Parameter settings for numerical test systems

Test number	Blockage type	l_1 (m)	l_2 (m)	l_3 (m)	l_4 (m)	R (m)	s	R_{L3} (m)	a_0 (m/s)	$\bar{a}_b$ (m/s)
T1	Blockage-free	300	100	100	500	0.25	0	0.25	1,206	1,206
T2	Uniform	300	100	100	500	0.25	0	0.20	1,206	1,249
T3	Nonuniform	300	100	100	500	0.25	1×10^{-3}	0.15	1,206	1,249
T4	Nonuniform	300	100	100	500	0.25	7.5×10^{-4}	0.175	1,206	1,238
T5	Nonuniform	300	100	100	500	0.25	5×10^{-4}	0.20	1,206	1,227
T6	Nonuniform	390	10	10	590	0.25	1×10^{-2}	0.15	1,206	1,249
T7	Nonuniform	399	1	1	599	0.25	1×10^{-1}	0.15	1,206	1,249

this study is to investigate the influence of blockage nonuniformity on resonant frequency shifts. Thus, only the linearized steady friction is included in the following numerical applications. The nonlinear steady friction and unsteady friction (Meniconi et al. 2014) can be also included using a method similar to the one presented in Duan et al. (2018).

Uniform and Nonuniform Blockages with Same Blocked Volume

To study the influence of blockage nonuniformity (blockage severity, length, and slope) on transient frequency responses, seven test cases (Tests T1–T7) with different parameters listed in Table 3 are investigated using the analytical results obtained in this study. In this section, the first three tests in Table 3 (i.e., T1–T3) are used for comparison of the impacts of pipe blockage and its nonuniformity on transient frequency responses. Specifically, Tests T2 and T3 are the cases of uniform and nonuniform blockages with same blocked volume in the pipeline, and Test T1 is the intact pipeline system.

The transient frequency responses at downstream end for these three tests are plotted in Fig. 7. Fig. 7(a) is shown for the relatively low frequency domain, in which the dimensionless frequency ω^* ranges from 0 to 20. As shown in Fig. 7(a), the resonant peaks

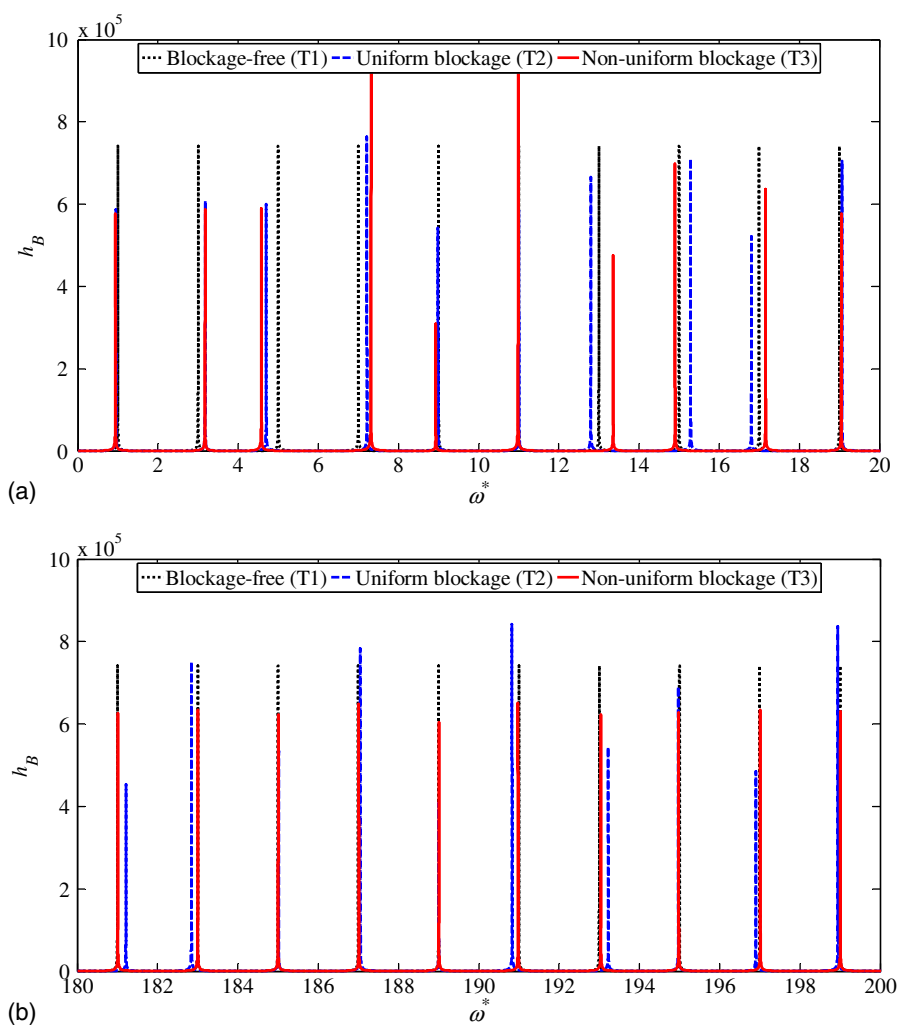

Fig. 7. Comparison of transient frequency responses for different pipe blockage situations with linearized steady friction effect: (a) low frequency mode domain; and (b) higher frequency mode domain.

Downloaded from ascelibrary.org by Hong Kong University of Sci and Tech (HKUST) on 06/05/19. Copyright ASCE. For personal use only; all rights reserved.

for the intact pipeline system are uniformly distributed in the frequency domain, whereas the presence of uniform and nonuniform blockages within the pipeline results in evident resonant frequency shifts and peak amplitude changes. Moreover, the resonant frequency shift and the peak amplitude change induced by uniform and nonuniform blockages have significant differences, although the same blockage volume has been imposed for the two blockage situations. Fig. 7(b) is plotted for the relatively higher frequency domain, with the dimensionless frequency ω^* from 180 to 200. Similar with low frequency modes, both the resonant frequency shift and peak amplitude change caused by the nonuniform blockage are very different from that caused by the uniform blockage. Nevertheless, the resonant frequency for the nonuniform blockage system almost coincides with that of the blockage-free system. This can be explained by the Special Case (3) of Eq. (28): the frequency shift induced by the nonuniform blockage becomes less evident for high resonant frequency.

To gain an insight into the blockage-induced frequency shift and amplitude change, the first 100 resonant peaks for the uniform and nonuniform blockage systems are further extracted and analyzed. The frequency shifts for uniform and nonuniform blockages are plotted in Fig. 8(a). Note that the blockage-induced frequency shift for the mth resonant peak is defined as $\delta\omega_m^* = \omega_{mb}^* - \omega_{mi}^*$, where ω_{mb}^* = frequency of mth resonant peak for the blocked pipeline system; and ω_{mi}^* = frequency of mth resonant peak for the intact pipeline system. It can be observed from Fig. 8(a) that both the uniform and nonuniform blockages induced resonant frequency shifts that fluctuate with the peak number (equivalent to frequency). Specifically, the frequency shift fluctuation induced by the uniform blockage almost keeps the same order of magnitude as the peak number increases, whereas that induced by the nonuniform blockage is highly dependent on frequency. In the results for nonuniform blockage, the frequency shift fluctuation becomes less evident (tends to zero) as frequency increases. Similarly, the blockage-induced resonant peak amplitude change for the mth resonant peak is defined as $\delta h_{B,m} = h_{B,mb} - h_{B,mi}$, where $h_{B,mb}$ = amplitude of mth resonant peak for the blocked pipeline system; and $h_{B,mi}$ = amplitude of mth resonant peak for the intact pipeline system. The resonant peak amplitude changes for uniform and nonuniform blockages are plotted in Fig. 8(b) for convenient comparison. Similar to frequency shift fluctuation, the resonant peak amplitude change fluctuation induced by the uniform blockage almost keeps the same order of magnitude, whereas that induced by the nonuniform blockage gradually decreases with frequency.

Influence of Nonuniform Blockage Severity

In this section, the influence of nonuniform blockage severity on transient frequency responses is investigated. As shown in Fig. 5(b), the length of the nonuniform blockage (l_2 and l_3) is fixed. The blockage severity is defined as $S = (R - R_{L3})/R$, and it is proportional to the slope s of the nonuniform blockage

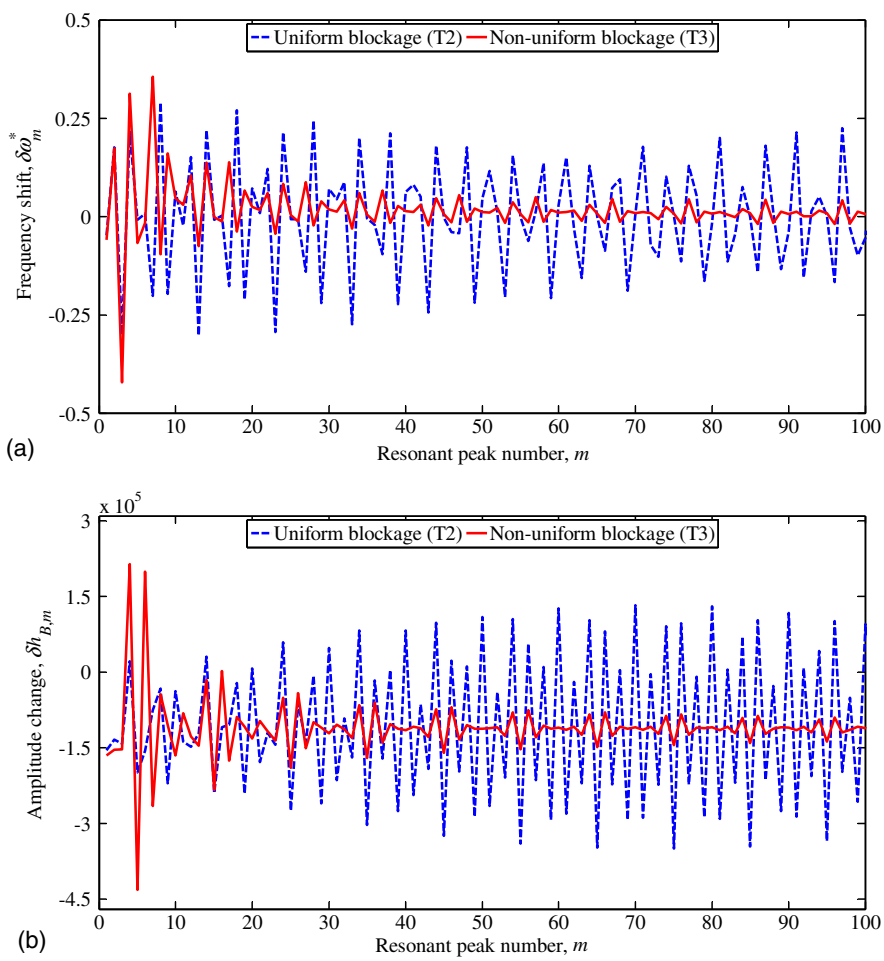

Fig. 8. Influence of uniform and nonuniform blockages on transient frequency responses: (a) relative resonant frequency shift; and (b) relative resonant peak amplitude change.

J. Hydraul. Eng., 2018, 144(8): 04018054

Downloaded from ascelibrary.org by Hong Kong University of Sci and Tech (HKUST) on 06/05/19. Copyright ASCE. For personal use only; all rights reserved.

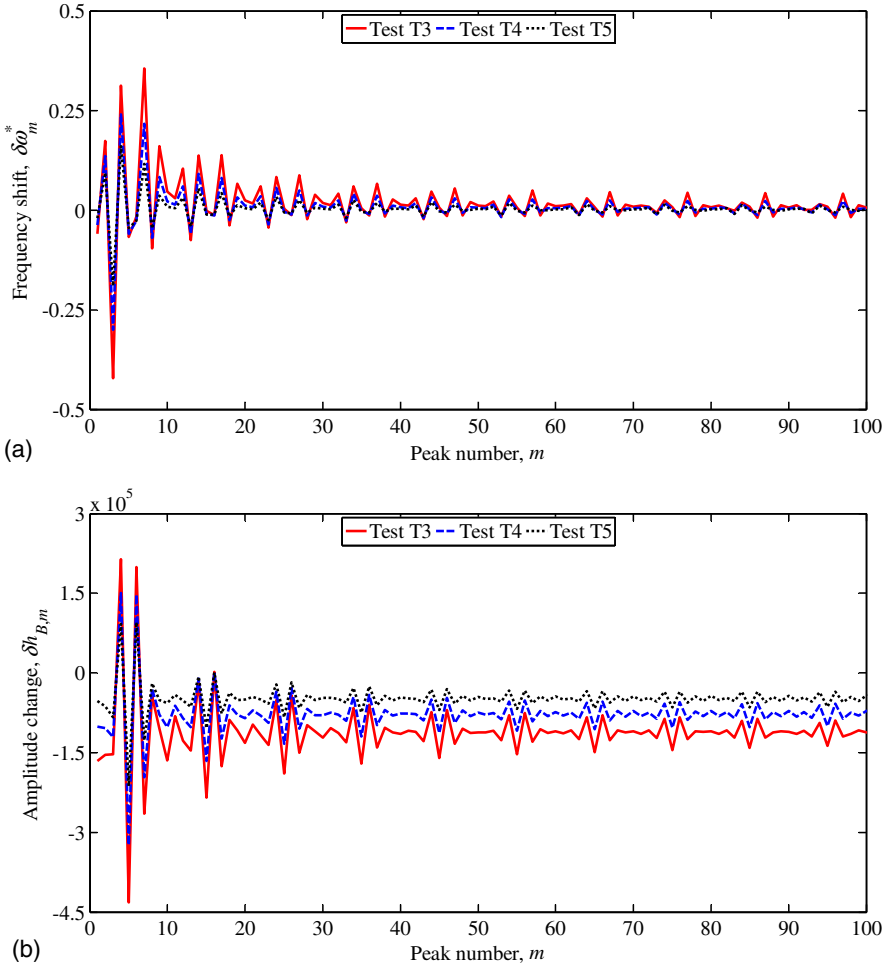

Fig. 9. Influence of nonuniform blockage with different blockage severities on transient frequency responses: (a) relative resonant frequency shift; and (b) relative resonant peak amplitude change.

$S \sim s = (R - R_{L3})/l_3$. For tests T3–T5 as shown in Table 3, R_{L3} gradually increases from 0.15 to 0.2 m, which means that the nonuniform blockage becomes less severe. The resonant frequency shift and peak amplitude change induced by nonuniform blockages are plotted in Fig. 9. It can be seen from Fig. 9(a) that the overall trend of frequency shift fluctuation for these cases is similar with Test T3 except for the extent of fluctuation. Specifically, the frequency shift fluctuation becomes less evident as the nonuniform blockage becomes less severe. Similarly, Fig. 9(b) shows that the extent of amplitude change fluctuation decreases as the nonuniform blockage becomes less severe. These results are reasonable because more severe nonuniform blockage should have more influence on the frequency and amplitude of transient frequency responses for an original intact pipeline system. In addition, the overall patterns (or trends) for frequency shift and amplitude change of these three cases are similar. This may indicate that the patterns of frequency shift and amplitude change are independent of the nonuniform blockage severity.

Influence of Nonuniform Blockage Length

The influence of nonuniform blockage length on transient frequency responses is examined herein by fixing other parameters. As is shown in Fig. 5(b), the location of nonuniform blockage center $(l_1 + l_2)$ and the pipe radius at the left boundary of Pipe 3 (R_{L3}) are fixed. The nonuniform blockage length (l_2 and l_3) gradually decrease from 100 to 1 m for Tests T3, T6, and T7 in Table 3. It is found that the frequency shift and amplitude change are in a certain pattern, and the period of this pattern is inversely proportional to the length of the nonuniform blockage. For convenient observation, the peak number m is divided by the normalized parameter L/l_2 and is expressed as m^* in Fig. 10.

Fig. 10(a) shows that the frequency shift patterns for three cases are periodic and roughly the same; meanwhile, the period of this induced pattern is in unit length of m^*. The overall extent of the frequency shift periodically decreases in terms of m^*. This frequency shift pattern can be explained by the former Special Case (3) of Eq. (28). As the m^*, which is proportional to ω, increases, the term $4R^2R_{L3}\omega^3\cos[k_b(l_1 + l_2 + l_3 + l_4)]$ containing ω^3 gradually becomes dominant and the frequency shift becomes less evident; thus, the overall extent of the periodic pattern gradually decreases. In addition, the periodic pattern can be attributed to the remaining trigonometric terms of Eq. (28). Similar behavior can be found in Fig. 10(b) for the amplitude change induced by the nonuniform blockage. Besides, a longer nonuniform blockage causes more amplitude attenuation.

Sensitivity Analysis of Resonant Frequency Shifts to the Wave Speed

In realistic pipelines as shown in Figs. 1(a and b), the wave speed $a_b(x)$ within the nonuniform blockage section would change along

Downloaded from ascelibrary.org by Hong Kong University of Sci and Tech (HKUST) on 06/05/19. Copyright ASCE. For personal use only; all rights reserved.

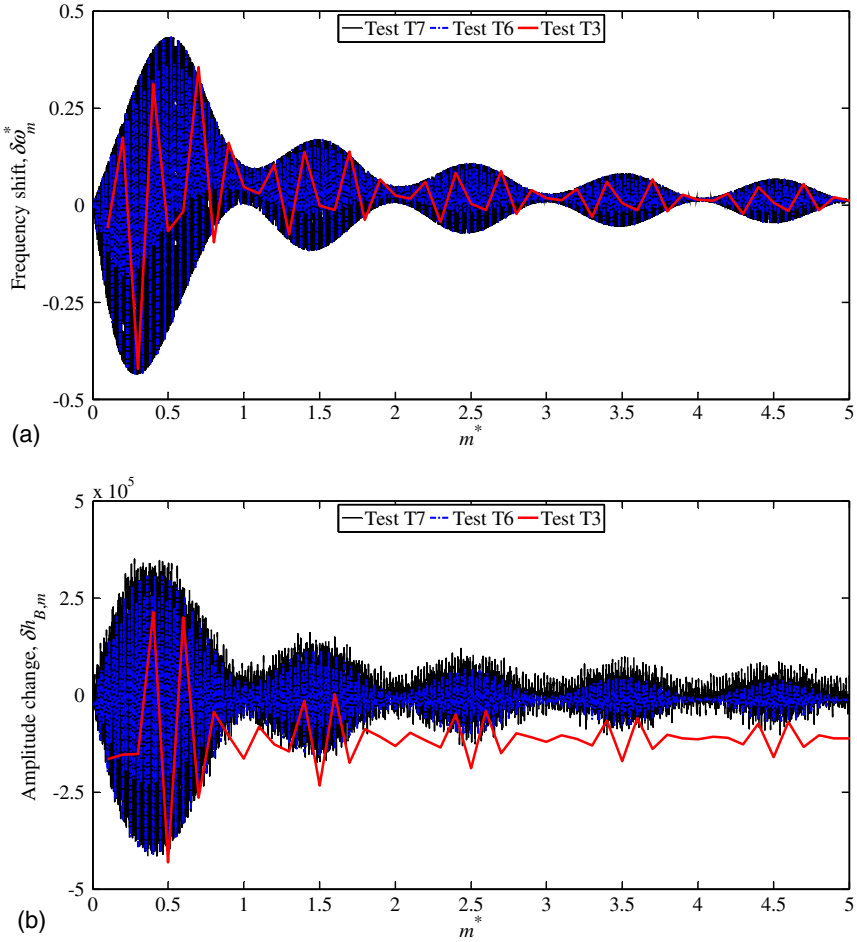

Fig. 10. Influence of nonuniform blockage with different blockage lengths on transient frequency responses: (a) relative resonant frequency shift; and (b) relative resonant peak amplitude change.

the axial direction due to the variation of pipe properties. In the preceding analytical derivations, $a_b(x)$ is represented approximately by the average wave speed $\bar{a}_b$ under the same blocked volume condition. As a result, the observed resonant frequency shifts in Tests T3–T7 are obtained based on this average wave speed $\bar{a}_b$. Therefore, it is necessary to examine the influence and validity range of this assumption for all tests in this study. For this purpose, the first-order second-moment (FOSM) method (Duan 2016) is adopted to theoretically investigate the sensitivity of the obtained resonant frequency shift patterns by the developed method in this study to the varying wave speed with average value of $\bar{a}_b$ in the nonuniform blockage section. Eq. (27) describes the relationship between the resonant frequency (ω_m) and system properties (e.g., average wave speed in the blocked section $\bar{a}_b$, wave speed in the intact section a_0, and slope of the nonuniform blockage s), which can be expressed as the following function:

$$\omega_m = G(\bar{a}_b, a_0, s, R, R_{L3}, l_2, \ldots) = G(X_1, X_2, X_3, \ldots, X_j) \tag{29}$$

where $G()$ = function; $X_1, \ldots, X_j$ = uncertainty factors; and j = number of uncertainty factors. The detailed procedures of FOSM for the sensitivity analysis may be found in the previous study by Duan (2016).

For quantitative analysis, the sensitivity coefficient of resonant frequency shifts to the average wave speed $\bar{a}_b$ for the mth resonant peak is defined as the variation (or variation percentage) of the transient response frequency shift to the variation (or variation percentage) of the wave speed

$$c_m = \frac{d(\delta\omega_m^*)}{da_b^*} = \frac{d(\delta\omega_m/\omega_{th})}{d(a_b/\bar{\alpha}_b)} \tag{30}$$

Eq. (30) is evaluated at $(\mu_1, \mu_2, \mu_3, \ldots, \mu_j)$, in which μ_1 through μ_j are mean values of variables X_1 through X_j.

By combining the results of Eqs. (27)–(30), the sensitivity coefficients (c_m) of Tests T3, T4, and T5 for the first 100 resonant peaks (representing both low and relatively high frequency domains) are calculated and plotted in Fig. 11(a). It can be observed in Fig. 11(a) that the first 20 resonant peaks (i.e., relatively low frequency domain), which are usually of practical importance, are less sensitive to the wave speed variation compared with remaining resonant peaks in high frequency regions, and the maximum value of sensitivity coefficient (i.e., 0.55) for the first 20 resonant peaks occurs at $m = 3$ for Test T5. Then, the sensitivity coefficients for two more severe blockage cases (i.e., Tests T3 and T4) gradually increase with frequency. The maximum value of sensitivity coefficient (i.e., 1.01) occurs at $m = 97$ for Test T3, which means that the maximum error (or uncertainty) of resonant frequency shifts induced by the varying wave speed is in the same order as the variation of wave speed parameter, whereas the sensitivity coefficients for the shallow blockage case (i.e., Test T5) almost keep the same order of magnitude in the frequency domain, which is much less than 1.0. As a result, the percentage errors of frequency shifts $\Delta\delta\omega_m^*$ induced

Downloaded from ascelibrary.org by Hong Kong University of Sci and Tech (HKUST) on 06/05/19. Copyright ASCE. For personal use only; all rights reserved.

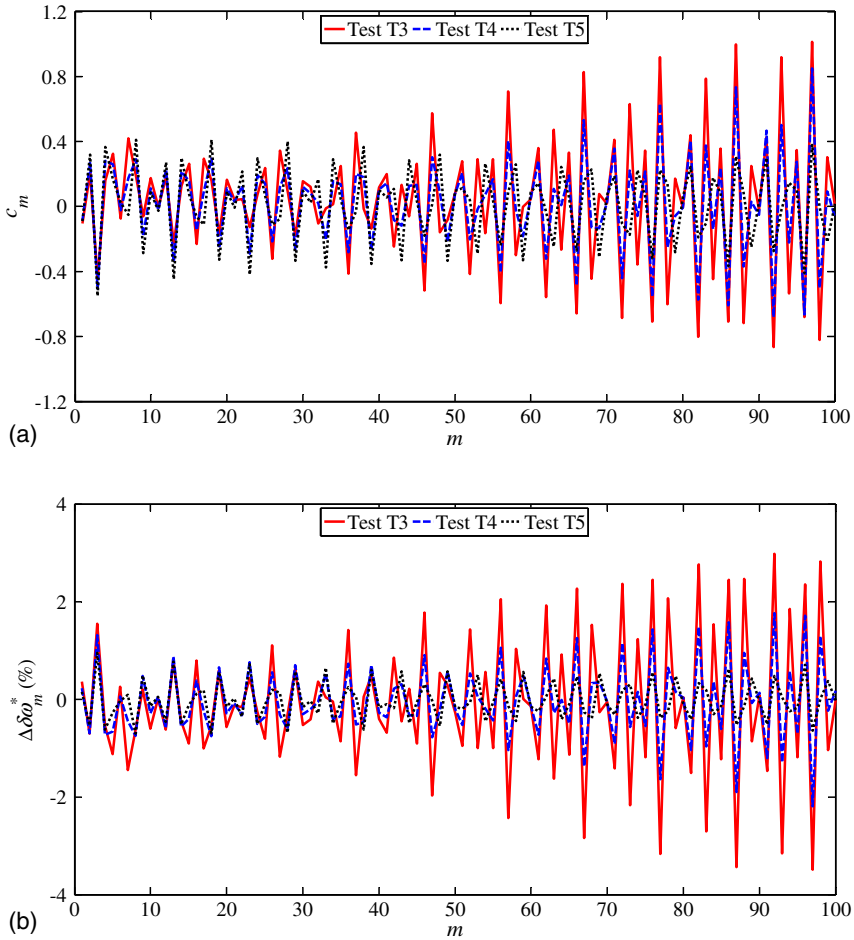

Fig. 11. (a) Sensitivity coefficients of resonant frequency shifts to the average wave speed within the blocked section; and (b) errors of resonant frequency shifts for Tests T3, T4, and T5.

by the varying wave speed in the blockage section for Tests T3, T4, and T5 are calculated as $\Delta\delta\omega_m^* = c_m((a_0 - \bar{a}_b)/\bar{a}_b) \times 100\%$ and plotted in Fig. 11(b). The result clearly shows that the maximum frequency shift errors for Tests T3, T4, and T5 are within 3.5, 2.2, and 1.0%, respectively, which are acceptable for the blockage detection application in this study.

Discussion and Implication

The preceding results and analysis suggest that, unlike the uniform blockage, the frequency shift $\delta\omega_m^*$ induced by the nonuniform blockage is frequency dependent, $\delta\omega_m^* \sim 1/\omega_m^*$. As the frequency ω_m^* increases, the induced frequency shift $\delta\omega_m^*$ becomes less evident. This finding is useful to explain the inaccuracy of the current frequency domain TBBDM, which is based on the blockage-induced frequency shift, for nonuniform blockages detection in Duan et al. (2017). Therefore, further improvement of such transient-based method is necessary for the nonuniform blockage detection.

The results comparison has also shown that, with fixed blockage length, the blockage-induced frequency shift gets more evident as the nonuniformity becomes more severe (i.e., $\delta\omega_m^* \sim s$). Besides, the overall extent of frequency shifts for different blockage severities is decreased as frequency increases (i.e., $\delta\omega_m^* \sim 1/\omega_m^*$). Therefore, for fixed blockage length, the blockage-induced frequency shift $\delta\omega_m^*$ is proportional to the slope of the nonuniform blockage (s) and is inversely related to the frequency ω_m^*, that is, $\delta\omega_m^* \sim s/\omega_m^*$. In addition, for fixed blockage severity, the frequency shift pattern for various blockage length is the same, and the period of this pattern T_{pattern} is inversely proportional to the length of the blockage $T_{\text{pattern}} \sim 1/l_2$. This period may offer us a method to detect the length of the nonuniform blockage. Based on $m/(L/l_2) = T(m^*)$, where $T = 1$ is the period of the frequency shift pattern in terms of m^*, the blockage length l_2 can be determined.

The obtained dependence relationship of transient wave behavior and blockage nonuniformity may provide useful implication to the transient analysis and blockage detection in real pipeline systems. Specifically, the current TBBDM can be further extended to more general and realistic situations of pipe blockages. That is, it is necessary to include the characteristic parameters, i.e., the slope (s), severity (R_{L3}), and location (l_4) of nonuniform blockages, in the TBBDM, which can be inversely determined based on the derived results of Eq. (27) in this study. Consequently, it is expected that, based on the results and findings of this study, the accuracy of current transient-based method can be improved and extended for realistic pipeline diagnosis, which will be investigated through further theoretical analysis and experimental tests in the next-step work.

It is worth noting that the wave equation, Eq. (1), used in this research is derived based on the classic 1D water hammer model in which the plane wave assumption has been imposed (Chaudhry 2014). As a result, the validity frequency range of this wave

Downloaded from ascelibrary.org by Hong Kong University of Sci and Tech (HKUST) on 06/05/19. Copyright ASCE. For personal use only; all rights reserved.

equation will be governed by the plane wave condition. According to previous studies on radial pressure waves (Che et al. 2018; Hall 1932; Louati and Ghidaoui 2017), the plane wave assumption is valid only when the harmonic frequencies are lower than the cut-off frequency of given pipe systems. On this point, all the peak frequencies used for analysis in this study are much smaller than this critical cut-off frequency of the blocked pipe systems. In other words, the used 1D wave equation is valid for all the results obtained in the present study. In addition, the average wave speed within nonuniform blockages in Table 3 is mainly evaluated from the changes of pipe diameters due to blockages. This is mainly because the main purpose of this study is to examine the influence of blockage nonuniformity on transient frequency responses. However, the developed method of this study is still valid for practical applications in which the wave speed varies with different factors, such as pipe diameters, wall thickness, and modulus of elasticity of the pipe wall, only if such information is known to the models.

Conclusions

This paper investigates the transient frequency responses for pressurized water pipeline systems with nonuniform blockages. The transient wave behavior is obtained by analytically solving the wave equation for a single blockage with a linearly varying diameter. The wave solution is used to derive the overall transfer matrix for a pressurized water pipeline system with nonuniform blockages, which is then numerically validated by the traditional MOC. With validated analytical results, the influences of blockage shape (slope), severity, and length on transient frequency responses are studied systematically for different cases. The results indicate the nonuniform blockage may induce very different modification patterns on the frequency shift and amplitude change of transient waves from the uniform blockage situation. The findings of this study are useful to improve the current transient-based method for nonuniform blockage detection in real pipeline systems. Although only the linear geometry of the nonuniform blockages has been considered in the current study, this research may provide a framework for exploring the diagnosis and analysis of realistic pipelines with nonuniform blockages. It is also noted that more investigations including numerical and experimental tests are required in the future work.

Acknowledgments

This research work was supported by the research grants from (1) the Hong Kong Research Grants Council (Projects Nos. T21-602/15-R, 25200616, and 15201017) and (2) the Hong Kong Polytechnic University (Projects Nos. 1-ZVCD and 1-ZVGF).

Notation

The following symbols are used in this paper:

$A = A(x)$ = pipe cross-sectional area (m^2);
$a = a(x)$ = wave speed (m/s);
a_0 = wave speed in intact pipelines (m/s);
$a_b = a_b(x)$ = wave speed within nonuniform blockages (m/s);
$\bar{a}_b$ = average wave speed within nonuniform blockages (m/s);
c_m = sensitivity coefficient;
g = gravitational acceleration (m/s^2);
h = pressure head deviation in the frequency domain (m);
$k = k(x) = \omega/a(x)$ = wave number (rad/m);
k_b = wave number for the nonuniform blockage (rad/m);
k_0 = wave number for the uniform blockage (rad/m);
L = total length of pipeline systems (m);
l_n = length of the nth nonuniform blockage (m);
m = peak number;
n = pipeline number;
P = instantaneous pressure in the time domain (Pa);
P_0 = mean pressure in the time domain (Pa);
p^* = pressure deviation from the P_0 (Pa);
p = pressure in the frequency domain (Pa);
q = discharge deviation in the frequency domain (m^3/s);
R = intact pipe radius (m);
R_{Ln} = pipe radius at the left boundary of the nth nonuniform blockage (m);
r_n = pipe radius of the nth nonuniform blockage (m);
$S = (R - R_{L3})/R$ = blockage severity;
$s_n = (R - R_{Ln})/l_n$ = slope of the nth nonuniform blockage;
t = time (s);
U_{ij} = elements of transfer matrix;
U^*_{ij} = elements of the overall transfer matrix for the four-pipeline system;
x = axial coordinate along the pipeline (m);
$\delta\omega^*_m$ = blockage-induced frequency shift for the mth resonant peak;
$\delta h_{B,m}$ = blockage-induced resonant peak amplitude change for the mth resonant peak (m);
ω = angular frequency (rad/s);
ω_{th} = fundamental frequency of the pipeline system (rad/s);
ω^* = nondimensional frequency;
ω^*_{mb} = frequency of mth resonant peak for the blocked pipeline system; and
ω^*_{mi} = frequency of mth resonant peak for the intact pipeline system.

References

Brunone, B. 1999. "Transient test-based technique for leak detection in outfall pipes." *J. Water Resour. Plann. Manage.* 125 (5): 302–306. https://doi.org/10.1061/(ASCE)0733-9496(1999)125:5(302).

Brunone, B., and M. Ferrante. 2001. "Detecting leaks in pressurised pipes by means of transients." *J. Hydraul. Res.* 39 (5): 539–547. https://doi.org/10.1080/00221686.2001.9628278.

Brunone, B., and M. Ferrante. 2004. "Pressure waves as a tool for leak detection in closed conduits." *Urban Water J.* 1 (2): 145–155. https://doi.org/10.1080/1573062042000271073.

Brunone, B., M. Ferrante, and S. Meniconi. 2008. "Discussion of 'detection of partial blockage in single pipelines' by P. K. Mohapatra, M. H. Chaudhry, A. A. Kassem, and J. Moloo." *J. Hydraul. Eng.* 134 (6): 872–874. https://doi.org/10.1061/(ASCE)0733-9429(2008)134:6(872).

Chaudhry, M. H. 2014. *Applied hydraulic transients*. 3rd ed. New York: Springer.

Che, T. C., H. F. Duan, P. J. Lee, S. Meniconi, B. Pan, and B. Brunone. 2018. "Radial pressure wave behavior in transient laminar pipe flows under different flow perturbations." *J. Fluids Eng.* 140 (10): 101203 https://doi.org/10.1115/1.4039711.

Colombo, A. F., P. J. Lee, and B. W. Karney. 2009. "A selective literature review of transient-based leak detection methods." *J. Hydro-Environ. Res.* 2 (4): 212–227. https://doi.org/10.1016/j.jher.2009.02.003.

Downloaded from ascelibrary.org by Hong Kong University of Sci and Tech (HKUST) on 06/05/19. Copyright ASCE. For personal use only; all rights reserved.

Covas, D., and H. Ramos. 2010. "Case studies of leak detection and location in water pipe systems by inverse transient analysis." *J. Water Resour. Plann. Manage.* 136 (2): 248–257. https://doi.org/10.1061/(ASCE)0733-9496(2010)136:2(248).

Covas, D., H. Ramos, N. Graham, and C. Maksimovic. 2004. "Application of hydraulic transients for leak detection in water supply systems." *Water Sci. Technol.: Water Supply* 4 (5–6): 365–374.

Datta, S., and S. Sarkar. 2016. "A review on different pipeline fault detection methods." *J. Loss Prevent. Proc.* 41 (May): 97–106. https://doi.org/10.1016/j.jlp.2016.03.010.

Duan, H. F. 2016. "Sensitivity analysis of a transient-based frequency domain method for extended blockage detection in water pipeline systems." *J. Water Resour. Plann. Manage.* 142 (4): 04015073. https://doi.org/10.1061/(ASCE)WR.1943-5452.0000625.

Duan, H. F. 2017. "Transient wave scattering and its influence on transient analysis and leak detection in urban water supply systems: Theoretical analysis and numerical validation." *Water* 9 (10): 789. https://doi.org/10.3390/w9100789.

Duan, H. F., T. C. Che, P. J. Lee, and M. S. Ghidaoui. 2018. "Influence of nonlinear turbulent friction on the system frequency response in transient pipe flow modelling and analysis." *J. Hydraul. Res.* 1–13. https://doi.org/10.1080/00221686.2017.1399936.

Duan, H. F., P. J. Lee, T. C. Che, M. S. Ghidaoui, B. W. Karney, and A. A. Kolyshkin. 2017. "The influence of non-uniform blockages on transient wave behavior and blockage detection in pressurized water pipelines." *J. Hydro-Environ. Res.* 17 (Dec): 1–7. https://doi.org/10.1016/j.jher.2017.08.002.

Duan, H. F., P. J. Lee, M. S. Ghidaoui, and J. Tuck. 2014. "Transient wave-blockage interaction and extended blockage detection in elastic water pipelines." *J. Fluids Struct.* 46 (Apr): 2–16. https://doi.org/10.1016/j.jfluidstructs.2013.12.002.

Duan, H. F., P. J. Lee, M. S. Ghidaoui, and Y. K. Tung. 2010. "Essential system response information for transient-based leak detection methods." *J. Hydraul. Res.* 48 (5): 650–657. https://doi.org/10.1080/00221686.2010.507014.

Duan, H. F., P. J. Lee, M. S. Ghidaoui, and Y. K. Tung. 2012. "Extended blockage detection in pipelines by using the system frequency response analysis." *J. Water Resour. Plann. Manage.* 138 (1): 55–62. https://doi.org/10.1061/(ASCE)WR.1943-5452.0000145.

Duan, H. F., J. L. Lu, A. A. Kolyshkin, and M. S. Ghidaoui. 2011. "The effect of random inhomogeneities of pipe cross-sectional area on wave propagation." In *Proc., 34th IAHR Congress*. Barton, Australia: Engineers Australia.

Ferrante, M., and B. Brunone. 2003. "Pipe system diagnosis and leak detection by unsteady-state tests. 1: Harmonic analysis." *Adv. Water Resour.* 26 (1): 95–105. https://doi.org/10.1016/S0309-1708(02)00101-X.

Gong, J., A. C. Zecchin, A. R. Simpson, and M. F. Lambert. 2014. "Frequency response diagram for pipeline leak detection: Comparing the odd and even harmonics." *J. Water Resour. Plann. Manage.* 140 (1): 65–74. https://doi.org/10.1061/(ASCE)WR.1943-5452.0000298.

Hall, W. M. 1932. "Comments on the theory of horns." *J. Acoust. Soc. Am.* 3 (4): 552–561. https://doi.org/10.1121/1.1915578.

James, W., and A. Shahzad. 2003. "Water distribution losses caused by encrustation and biofouling: Theoretical study applied to Walkerton, ON." In *Proc., World Water & Environmental Resources Congress 2003*. Reston, VA: ASCE.

Kim, S. H. 2017. "Multiple leakage function for a simple pipeline system." *Water Resour. Manage.* 31 (9): 2659–2673. https://doi.org/10.1007/s11269-017-1650-5.

Lee, P. J., H. F. Duan, M. S. Ghidaoui, and B. W. Karney. 2013. "Frequency domain analysis of pipe fluid transient behaviour." *J. Hydraul. Res.* 51 (6): 609–622. https://doi.org/10.1080/00221686.2013.814597.

Lee, P. J., H. F. Duan, J. Tuck, and M. S. Ghidaoui. 2015. "Numerical and experimental study on the effect of signal bandwidth on pipe assessment using fluid transients." *J. Hydraul. Eng.* 141 (2): 04014074. https://doi.org/10.1061/(ASCE)HY.1943-7900.0000961.

Lee, P. J., M. F. Lambert, A. R. Simpson, J. P. Vítkovský, and J. A. Liggett. 2006. "Experimental verification of the frequency response method for pipeline leak detection." *J. Hydraul. Res.* 44 (5): 693–707. https://doi.org/10.1080/00221686.2006.9521718.

Lee, P. J., J. Tuck, M. Davidson, and R. May. 2017. "Piezoelectric wave generation system for condition assessment of field water pipelines." *J. Hydraul. Res.* 55 (5): 721–730. https://doi.org/10.1080/00221686.2017.1323805.

Lee, P. J., J. P. Vitkovsky, M. F. Lambert, A. R. Simpson, and J. A. Liggett. 2008. "Discrete blockage detection in pipelines using the frequency response diagram: Numerical study." *J. Hydraul. Eng.* 134 (5): 658–663. https://doi.org/10.1061/(ASCE)0733-9429(2008)134:5(658).

Lee, P. J., J. P. Vítkovský, M. F. Lambert, A. R. Simpson, and J. A. Liggett. 2007. "Leak location in pipelines using the impulse response function." *J. Hydraul. Res.* 45 (5): 643–652. https://doi.org/10.1080/00221686.2007.9521800.

Louati, M., and M. S. Ghidaoui. 2017. "High-frequency acoustic wave properties in a water-filled pipe. 1: Dispersion and multi-path behaviour." *J. Hydraul. Res.* 55 (5): 613–631. https://doi.org/10.1080/00221686.2017.1354931.

Louati, M., S. Meniconi, M. S. Ghidaoui, and B. Brunone. 2017. "Experimental study of the eigenfrequency shift mechanism in a blocked pipe system." *J. Hydraul. Eng.* 143 (10): 04017044. https://doi.org/10.1061/(ASCE)HY.1943-7900.0001347.

Meniconi, S., B. Brunone, and M. Ferrante. 2010. "In-line pipe device checking by short-period analysis of transient tests." *J. Hydraul. Eng.* 137 (7): 713–722. https://doi.org/10.1061/(ASCE)HY.1943-7900.0000309.

Meniconi, S., B. Brunone, M. Ferrante, and C. Massari. 2011. "Small amplitude sharp pressure waves to diagnose pipe systems." *Water Resour. Manage.* 25 (1): 79–96. https://doi.org/10.1007/s11269-010-9688-7.

Meniconi, S., H. F. Duan, B. Brunone, M. S. Ghidaoui, P. J. Lee, and M. Ferrante. 2014. "Further developments in rapidly decelerating turbulent pipe flow modeling." *J. Hydraul. Eng.* 140 (7): 04014028. https://doi.org/10.1061/(ASCE)HY.1943-7900.0000880.

Meniconi, S., H. F. Duan, P. J. Lee, B. Brunone, M. S. Ghidaoui, and M. Ferrante. 2013. "Experimental investigation of coupled frequency and time-domain transient test-based techniques for partial blockage detection in pipelines." *J. Hydraul. Eng.* 139 (10): 1033–1040. https://doi.org/10.1061/(ASCE)HY.1943-7900.0000768.

Munjal, M. L. 2014. *Acoustics of ducts and mufflers*. New York: Wiley.

Rubio Scola, I., G. Besançon, and D. Georges. 2017. "Blockage and leak detection and location in pipelines using frequency response optimization." *J. Hydraul. Eng.* 143 (1): 04016074. https://doi.org/10.1061/(ASCE)HY.1943-7900.0001222.

Sattar, A. M., and M. H. Chaudhry. 2008. "Leak detection in pipelines by frequency response method." Supplement, *J. Hydraul. Res.* 46 (S1): 138–151. https://doi.org/10.1080/00221686.2008.9521948.

Sattar, A. M., M. H. Chaudhry, and A. A. Kassem. 2008. "Partial blockage detection in pipelines by frequency response method." *J. Hydraul. Eng.* 134 (1): 76–89. https://doi.org/10.1061/(ASCE)0733-9429(2008)134:1(76).

Stephens, M. L. 2008. "Transient response analysis for fault detection and pipeline wall condition assessment in field water transmission and distribution pipelines and networks." Ph.D. thesis, Univ. of Adelaide.

Tuck, J., P. J. Lee, M. Davidson, and M. S. Ghidaoui. 2013. "Analysis of transient signals in simple pipeline systems with an extended blockage." *J. Hydraul. Res.* 51 (6): 623–633. https://doi.org/10.1080/00221686.2013.814599.

Wang, X. J., M. F. Lambert, and A. R. Simpson. 2005. "Detection and location of a partial blockage in a pipeline using damping of fluid transients." *J. Water Resour. Plann. Manage.* 131 (3): 244–249. https://doi.org/10.1061/(ASCE)0733-9496(2005)131:3(244).

Webster, A. G. 1919. "Acoustical impedance and the theory of horns and of the phonograph." *Proc. Natl. Acad. Sci.* 5 (7): 275–282. https://doi.org/10.1073/pnas.5.7.275.

Wylie, E. B., V. L. Streeter, and L. Suo. 1993. *Fluid transients in systems*. Englewood Cliffs, NJ: Prentice Hall.

Downloaded from ascelibrary.org by Hong Kong University of Sci and Tech (HKUST) on 06/05/19. Copyright ASCE. For personal use only; all rights reserved.